14th International Conference on Structural Safety and Reliability - ICOSSAR'25
1-6 June, 2025 - Los Angeles California, USA
R. Ghanem, E. Johnson, S. Masri and A. Olivier (Eds)

SYSTEM EFFECTS IN TIMBER CONNECTIONS COMPRISING MULTIPLE FASTENERS

ALEX SIXIE CAO[1], SEBASTIAN THÖNS[2], ROBERT JOCKWER[3] AND PEDRO PALMA[4]

[1] Empa - Swiss Federal Institute of Materials Science and Technology, Structural Engineering Research Laboratory
Ueberlandstrasse 129, 8600 Dübendorf, Switzerland
alex.cao@empa.ch

[2] LTU, Lund University, Division of Structural Engineering
John Ericssons väg 1, SE-221 00 Lund, Sweden
sebastian.thons@kstr.lth.se

[3] TUD, Dresden University of Technology
George-Bähr-Str. 1, 01069 Dresden, Germany
robert.jockwer@tu-dresden.de

[4] Empa - Swiss Federal Institute of Materials Science and Technology, Structural Engineering Research Laboratory
Ueberlandstrasse 129, 8600 Dübendorf, Switzerland
pedro.palma@empa.ch

Key words: Timber connections, System reliability, Richard-Abbott, Group effects, Slip modulus

Abstract. Timber connections often comprise multiple fasteners, leading to group effects where the connection behaviour deviates from the sum of its individual components. EN 1995-1-1:2004 accounts for the group effects in the load-carrying capacity using an effective number of fasteners following a power law, which was derived from experiments on laterally-loaded single- and multiple-fastener connections. However, it has been criticized for not distinguishing between statistical scale effects and brittle failure modes from mechanics, which may lead to unsafe designs. In the ultimate limit state, EN 1995-1-1:2004 uses the rigid-plastic European yield model and assumes an ultimate secant stiffness $K_{\mathrm{u}} = \frac{2}{3}K_{\mathrm{ser}}$ based on ambiguously defined displacement limits, where K_{ser} is the slip modulus for serviceability considerations. However, it is unclear if the secant stiffness in EN 1995-1-1:2004 is compatible with the rigid-plastic assumption. This paper investigates group effects in timber connections using mechanical and probabilistic modelling focusing on failure mode III with two plastic hinges per shear plane in laterally-loaded dowel fasteners. The results revealed that the effective number of fasteners followed a linear trend and that the connections exhibited homogenization effects with reduced scatter for an increasing number of fasteners. Furthermore, the existing approach of $K_{\mathrm{u}} = \frac{2}{3}K_{\mathrm{ser}}$ was found to be too stiff and that $K_{\mathrm{u}} = \frac{1}{6}K_{\mathrm{ser}}$ is more appropriate. However, this may lead to premature brittle failure modes from larger fastener displacements, which may necessitate stricter or larger minimum spacing requirements.

1 INTRODUCTION

1.1 Background

Timber connections with metallic fasteners often provide the ductility in timber structures [16] and are frequently governing the design. They often comprise multiple metallic fasteners, such as laterally-loaded dowels, nails, and bolts. Despite their importance, the behaviour of timber connections is often considered using simplified methods that may not always reflect their mechanical behaviour.

1.1.1 Single laterally-loaded dowel-type fasteners

The load-carrying capacity of laterally-loaded dowel-type fasteners, such as nails, screws, bolts, and dowels, is often considered using the European Yield Model (EYM) [14, 18]. It is a rigid-plastic model that predicts the load-carrying capacity based on distinct failure modes, which, for a connection with a single slotted-in steel plate and a single laterally-loaded fastener per shear plane are:

$$r = \min \begin{cases} \text{Mode I:} & f_{\mathrm{h}} t d, \\ \text{Mode II:} & f_{\mathrm{h}} t d \left(\sqrt{2 + \frac{4 M_{\mathrm{y}}}{f_{\mathrm{h}} d t^2}} - 1 \right), \\ \text{Mode III:} & 2 \sqrt{M_{\mathrm{y}} f_{\mathrm{h}} d}, \end{cases} \tag{1}$$

where f_{h} is the timber embedment strength, t thickness of the timber side member, d diameter of the fastener, and M_{y} is the yield moment of the fastener [7]. In mode I, the resistance r is governed by embedment failure of the timber. In mode II, resistance r is provided by one plastic hinge in the fastener per shear plane. In mode III, two plastic hinges in the fastener per shear plane develop simultaneously. The most ductile failure is developed in mode III and often requires slender fasteners.

Despite the widespread adoption of the EYM, it is a pure capacity model and is therefore limited related to its inability to consider stiffness. Besides, it does not explicitly address brittle failure modes within the timber, which can occur before any of the failure modes in Equation 1 are activated [17].

1.1.2 Multiple laterally-loaded dowel-type fasteners

When multiple fasteners are used in a connection, the behaviour of the group $R(\delta)$ cannot be determined by multiplying the behaviour of a single fastener $r(\delta)$ with the number of fasteners n, where δ is a displacement. Geometry of the connection, overlapping stresses, ductility of the single fasteners, manufacturing tolerances, misalignments, and material scatter contribute to the group behaviour generally not being proportionate to that of a single fastener $R(\delta) \not\propto r(\delta)$.

The scaling between a single fastener $r(\delta)$ and multiple fasteners $R(\delta)$ can be accounted for using the concept of an "effective number of fasteners" n_{ef}, where the group behaviour can be defined as:

$$R(\delta) = n_{\mathrm{ef}} r(\delta), \quad n_{\mathrm{ef}} \leq n, \tag{2}$$

where n is the number of fasteners. The effective number of fasteners n_{ef} in Equation 2 assumes ductile behaviour and is usually reserved for capacity considerations. However, manufacturing tolerances, misalignments, and material scatter also influence the initial loading phase, which may be critical for serviceability considerations. With enough fastener ductility, low manufacturing tolerances and misalignments are less influential on the capacity from load redistribution effects [3].

Table 1: Effective number of fasteners n_{ef}, where CLT is cross-laminated timber and a_1 the fastener spacing parallel to the grain. †Based on Jorissen [[15]]: $n_{\mathrm{ef}} = n^{0.9}\sqrt[4]{\frac{a_1}{10d}}$. ††If block shear is avoided. †††λ_{y} is the yield slenderness and λ_{ef} the effective slenderness of the dowel.

Reference	n_{ef}	Scope
EN 1995-1-1:2004† [7]	$n^{0.9}\sqrt[4]{\frac{a_1}{14d}}$	laterally-loaded bolts and dowels parallel to the grain
	$n^{0.9}$	laterally-loaded screws
Plüss and Brandner (2014) [20] Brandner et al. [1]	$0.90n^{\dagger}$	Axially loaded self-tapping screws in the CLT side face
Ringhofer et al. [22]	$n^{\dagger\dagger}$	laterally-loaded dowel-type fasteners in the CLT side face
Hossain et al. [11]	Monotonic capacity: $0.9n$ Cyclic capacity: $n^{0.9}$ Stiffness: $n^{0.8}$ Ductility: $n^{0.9}$	Self-tapping screws in CLT
Gehri et al. [9]	$n_{\mathrm{ef}} = 2\left(\frac{n}{2}\right)^{0.8\lambda_{\mathrm{r}}},\ \lambda_{\mathrm{r}} = \frac{\lambda_{\mathrm{ef}}}{\lambda_{\mathrm{y}}}$ †††	laterally-loaded dowels parallel to grain with ductile behaviour

There are several expressions of the effective number of fasteners n_{ef}, some of which are presented in Table 1. The number of effective fasteners n_{ef} is largely empirically determined from experiments on a relatively small number of fasteners n, which may not be representative of modern connections with a large number of fasteners n. Furthermore, the effective number of fasteners n_{ef} implicitly combines statistical and mechanical effects that can trigger brittle failure modes, such as splitting, row shear, block shear, and net tension failure. This may be non-conservative if the brittle failure modes are triggered before the ductile modes II and III in Equation 1 can develop [13]. As such, brittle failure modes should be treated separately [24]. Brittle failure modes are usually avoided through sufficient minimum spacing a_1 between the fasteners, end or edge distances, and the timber thickness t, and is also enforced by prescriptive rules in EN 1995-1-1:2004 [7]. However, adherence to the prescriptive requirements in EN 1995-1-1:2004 [7] does not definitively exclude brittle failure modes in complex loading situations or when having many fasteners.

1.1.3 Stiffness of fasteners and connections

Timber connections are often flexible and idealized as pinned, resulting in their design as pure shear connections. However, the modelling idealization fails to account for bending moments that occur in semi-rigid connections, which may lead to premature failure from complex loading states. A typical resistance curve $R(\delta)$ of a group of fasteners $R(\delta)$ can be described by [12]: (i) initial phase with low and increasing stiffness from tolerances and misalignments; (ii) quasi-linear phase where all components are activated; (iii) non-linear yielding phase with the development of plasticity and ductile failure modes; (iv) quasi-linear post-yield phase with hardening or softening before failure.

Design standards idealize the non-linear connection behaviour using simplified stiffnesses. For serviceability considerations, a slip modulus K_{ser} is defined for an individual fastener and the connection behaviour is $K_{\mathrm{y}} = nK_{\mathrm{ser}}$ [7]. The slip modulus $K_{\mathrm{ser}} = \rho_{\mathrm{mean}}^{1.5}d/23$ is an empirically derived

mean value and a function of the mean timber density ρ_{mean} and fastener diameter d. It is based on $0.4r_{\text{u,k}}$ [5], where $r_{\text{u,k}}$ is the characteristic ultimate load of a fastener. However, the slip moduli K_{ser} in EN 1995-1-1:2004 [7] may be unsuitable for modern timber connections [12].

In the ultimate limit state, EN 1995-1-1:2004 [7] provides an ultimate slip modulus K_{u} that is simply defined as $K_{\text{u}} = \frac{2}{3}K_{\text{ser}} \therefore K_{\text{s,u}} = n\frac{2}{3}K_{\text{ser}}$, where $K_{\text{s,u}}$ is the secant stiffness of the connection. However, it is not clear if the ultimate slip modulus K_{u} should be considered as the secant between zero load and the maximum load r_u or at failure defined as $0.80r_u$ [12]. Moreover, it was determined from nailed connections, that may not be representative of contemporary timber structures, at ambiguous deformations [4, 12]. The use of the ultimate slip modulus $K_{\text{u}} = \frac{2}{3}K_{\text{ser}}$ may also be unsafe when considering load-redistribution mechanisms that depend on component or connection stiffnesses [12].

The initial K_{ser} and ultimate K_{u} slip moduli in EN 1995-1-1:2004 [7] are substantial simplifications of the non-linear behaviour $r(\delta)$. They are based on mean values and do not consider the variability. Furthermore, direct linear scaling of the stiffness parameters $K_x = \sum_n k_i$ is assumed in the serviceability and ultimate limit states, where K_x is the stiffness of a group of fastener, k_i the stiffness of a single fastener, and n the number of fasteners. This neglects the effects from manufacturing tolerances, misalignments, and material scatter.

1.2 Objectives and scope

The objective of this study is to assess the system effects in timber connections through mechanical and probabilistic modelling of the full non-linear resistance curve $R(\delta)$. This enables reliability analyses for any quantity of interest along and between points at the non-linear resistance curve $R(\delta)$. Thus, group effects can be considered for any stiffness and resistance quantities.

The scope is timber connections with laterally-loaded dowel fasteners and a slotted-in steel plate without initial slip and brittle failure modes. The modelling considers experimentally calibrated parametric resistance curves based on the dataset by Palma and Wydler [19], and only includes the ductile failure mode III in the EYM of the individual fasteners. Other failure modes are not included in the present study but are identified as important future topics. The research contributes to developing design rules based on explicit probabilistic physical modelling, which may lead to a more coherent reliability between the failure modes of timber connections and improved mechanical representation.

2 MECHANICAL MODEL

The fastener behaviour $r(\delta)$ is idealized using the parametric Richard-Abbott material model [21]:

$$r(\delta) = \left(\frac{k_{\text{e}} - k_{\text{p}}}{\left(1 + \left(\frac{k_{\text{e}} - k_{\text{p}}}{r_{\text{int}}}\right)^{a}\right)^{\frac{1}{a}}} + k_{\text{p}} \right) \delta, \tag{3}$$

where k_{e} is the initial tangent stiffness, k_{p} is the inelastic or plastic tangent stiffness, r_{int} is the resistance intersection between the initial k_{e} and plastic k_{p} tangent stiffnesses, and a is a model parameter that controls the transition between the tangents. The ultimate displacement δ_{u} is used as the failure criterion for the individual fasteners $r_i(\delta)$. To scale the behaviour of individual fasteners $r(\delta)$ to a fastener group $R(\delta)$, a mechanical model [2] is used. For axial loading, the group behaviour $R(\delta)$ is:

$$R(\delta) = \sum_{i=1}^{n} r_i(\delta), \tag{4}$$

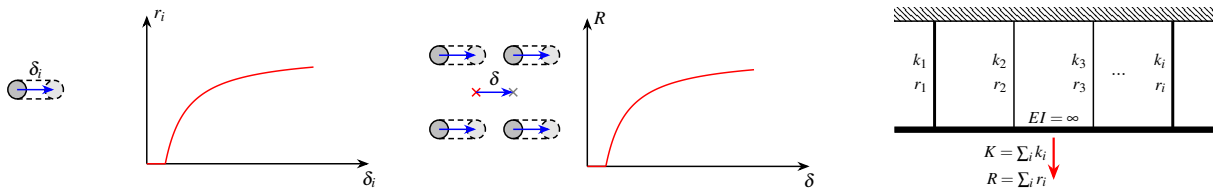

(a) Fastener resistance $r(\delta)$. (b) Connection resistance $R(\delta)$. (c) Mechanical model.

Figure 1: Mechanical model of a connection with multiple fasteners.

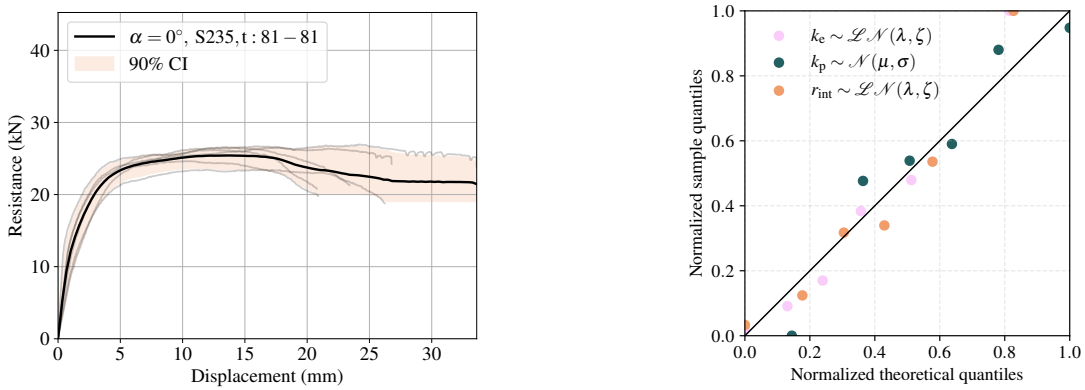

(a) Experimental results $r(\delta)$. (b) Normalized QQ-plot.

Figure 2: Experimental data from Palma and Wylder [19] and a normalized QQ-plot comparing the assumed distributions and calibrated Richard-Abbott [21] model parameters.

where n is the number of fasteners and $r_i(\delta)$ is the individual fastener behaviour in Equation 3. Equation 4 assumes a redundant system [3, 10] with displacement-compatibility δ between the ductile fasteners i, shown in Figure 1, instantaneous redistribution of loads, and no correlation between the fasteners i. However, each fastener can have a unique behaviour $r_i(\delta)$, as shown in Figure 1.

3 MATERIALS AND METHOD

3.1 Materials

Palma and Wydler [19] conducted experiments on single-fastener timber connections with a laterally-loaded dowel and slotted-in steel plate targeting mode III in Equation 1. The timber comprised $t = 81$ mm Norway spruce laminated veneer lumber (*Picea abies* (L.) H. Karst) without cross veneers [23]. The timber was pre-conditioned according to EN 26891:1991 [6] under 65 % relative humidity and 20 °C. The dowels comprised S235 bright drawn mild steel bars with circular cross-sections and a diameter $d = 10$ mm, with a mean yield strength $f_y = 583$ N/mm^2 ($cov = 0.08$) and elastic modulus $E_{mean} = 199$ kN/mm^2 ($cov = 0.11$). The results of the six specimens on single-fastener connections in tension parallel to the grain $\alpha = 0$ ° [19] without initial slip are shown in Figure 2a, where the shaded area is the 90 % confidence interval computed from the coefficient of variation cov at each displacement δ, thick black line is the mean, and gray thin lines the individual specimens.

Table 2: Richard-Abbott [21] model parameters calibrated to the single-fastener experiments by Palma and Wydler [19]. Coefficients of variation cov are given in the parentheses.

Parameter	k_e (kN/mm)	k_p (kN/mm)	r_int (kN)	a $(-)$	d_u (mm)	r_u (kN)
Mean (cov)	20.2 (0.42)	-0.4 (0.67)	36.3 (0.17)	1 (0.00)	25.3 (0.17)	21.5 (0.09)

Table 3: Correlation matrix of the random variables X_i of the Richard-Abbott [21] model parameters.

X_i	k_e	k_p	r_int	δ_u	r_u
k_e	1	0.79	-0.76	0.81	0.80
k_p		1	-0.99	0.79	0.73
r_int			1	-0.74	-0.64
δ_u				1	0.61
r_u					1

3.2 Method

The Richard-Abbott [21] model parameters in Equation 3 were calibrated to each of the experiments with $a = 1$ and the correlation matrix was computed. A lognormal distribution $\mathcal{LN}(\lambda, \zeta)$ was assumed for the initial tangent stiffness k_e, normal distribution $\mathcal{N}(\mu, cov)$ for the plastic tangent stiffness k_p, and a lognormal distribution $\mathcal{LN}(\lambda, \zeta)$ for the resistance intersection between the tangent stiffnesses r_int, where μ is the mean, $cov = \sigma/\mu$ coefficient of variation, and σ the standard deviation. Figure 2b shows a normalized QQ-plot of the assumed distributions and the Richard-Abbott [21] parameters. For each connection with $n \in [1, 3, 5, 15, 30, 60, 90]$ fasteners, 10^4 correlated random realizations were generated with the correlation matrix and assumed distributions using copulas.

4 RESULTS AND DISCUSSION

4.1 Single fastener

The results of the calibration of the Richard-Abbott [21] model parameters to the single-fastener experiments by Palma and Wydler [19] are shown in Table 2. The correlation matrix between the model parameters of the Richard-Abbott model [21] is shown in Table 3 and generally shows strong correlation between the parameters with the correlation coefficients $|\rho_{X_i X_j}| \not\approx 0$.

4.2 Multiple fasteners

4.2.1 Resistance curves

The resistance curves $R(\delta)$ for $n \in [5, 90]$ fasteners are shown in Figure 3a and 3b. For a small connection, each fastener failure is reflected in the step-wise shape of the confidence interval in Figure 3a. Barring the softening phase, the widest confidence band is in the transition between the elastic and inelastic states, and the narrowest in the initial phase. More fasteners $n \to \infty$ leads to a smoother and narrower confidence band, showing a beneficial homogenization effect and a smaller coefficient of variation cov when using more fasteners n in a connection. This may enable the use of lower partial safety factors γ_M for connections with many fasteners n in semi-probabilistic design, potentially enabling more efficient reliability-based designs and more predictable connection behaviour.

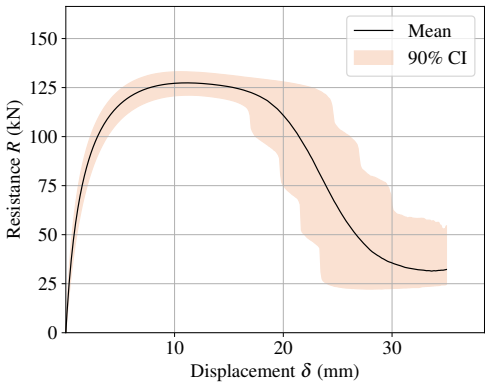

(a) $n = 5$.

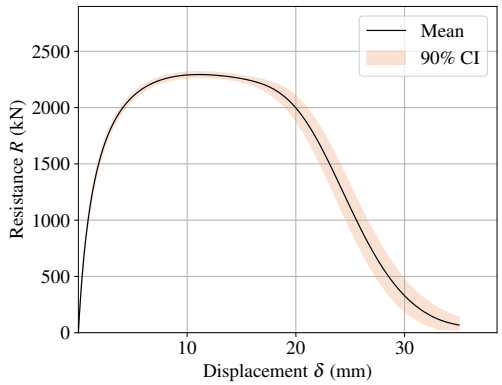

(b) $n = 90$.

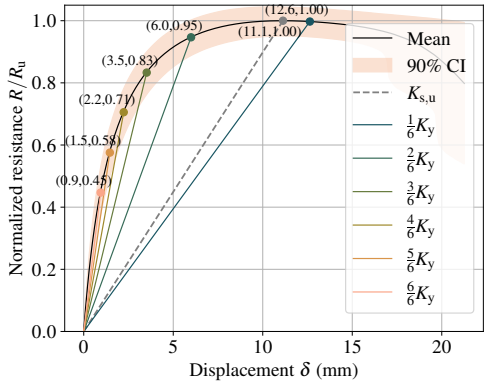

(c) $n = 5$.

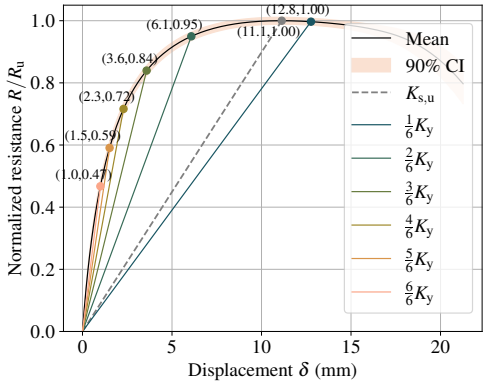

(d) $n = 90$.

Figure 3: (a) and (b): resistance curves $R(\delta)$ with fasteners n; (c) and (d): truncated normalized resistance curves $R(\delta)/R_{\mathrm{u}}$ with fasteners n showing secant stiffnesses xK_{y}, where $x \in [\frac{1}{6}, \frac{2}{6}, \frac{3}{6}, \frac{4}{6}, \frac{5}{6}, \frac{6}{6}]$.

4.2.2 Probabilistic distributions

Table 4 shows the probabilistic distributions that had the overall best fit for the quantities of interest $P \in [K_{\mathrm{y}}, K_{\mathrm{s,u}}, R_{\mathrm{y}}, R_{\mathrm{u}}]$. As in Figure 3, the reduced scatter with more fasteners n is also reflected in the coefficient of variation cov in Table 4. The scatter in the stiffness parameters K_{y} and $K_{\mathrm{s,u}}$ is generally higher than for the capacity parameters R_{y} and R_{u}. Consequently, the capacity-governed limit states would require smaller partial safety factors γ_{M} than the stiffness-governed limit states.

4.2.3 Group effects

Group effects on the connection scale were assessed by generalizing Equation 2:

$$n_{\mathrm{ef}}(P(n)) = \frac{P(n)}{P(n=1)}, \tag{5}$$

where $P \in [K_{\mathrm{y}}, K_{\mathrm{s,u}}, R_{\mathrm{y}}, R_{\mathrm{u}}]$ is a quantity of interest, n the number of fasteners, K_{y} the elastic stiffness, $K_{\mathrm{s,u}}$ the secant stiffness to the ultimate or maximum load-carrying capacity R_{u}, and R_{y} the yield capacity of the connection. The elastic stiffness K_{y} was determined from the secant between the $10\ \%$ and $40\ \%$ points of the maximum load-carrying capacity R_{u}, and the yield capacity R_{y} from

Table 4: Proposed probabilistic distributions of the quantities of interest $P \in [K_{\mathrm{y}}, K_{\mathrm{s,u}}, R_{\mathrm{y}}, R_{\mathrm{u}}]$.

Parameter	Distribution	cov for $n \in [1, 3, 5, 10, 15, 30, 60, 90]$							
		1	3	5	10	15	30	60	90
K_{y}	$\mathcal{LN}(\lambda, \zeta)$	0.33	0.20	0.15	0.11	0.09	0.06	0.04	0.03
$K_{\mathrm{s,u}}$	$\mathcal{W}(c, \lambda, \theta)$	0.27	0.14	0.10	0.07	0.05	0.04	0.03	0.02
R_{y}	$\mathcal{LN}(\lambda, \zeta)$	0.07	0.04	0.04	0.03	0.02	0.01	0.01	0.01
R_{u}	$\mathcal{W}(c, \lambda, \theta)$	0.08	0.04	0.03	0.02	0.02	0.01	0.01	0.01

the intersection between the elastic secant K_{y} and a tangent $\frac{1}{6}K_{\mathrm{y}}$ on the resistance curve according to EN 12512:2001 [8]. With Equation 5, the group effect was quantified through the effective number of fasteners n_{ef} for the different quantities of interest P.

Figure 4 shows parity plots between the number of fasteners n and the effective number of fasteners n_{ef} using Equation 5 for the quantities of interest P. The observed relation between the effective number of fasteners n_{ef} and actual number of fasteners n is mainly linear. This is contrary to Jorissen [15] and EN 1995-1-1:2004 [7], which uses a power law $n_{\mathrm{ef}} = n^{0.9}$ that disproportionately penalizes the use of many fasteners in a connection. However, Jorissen and EN 1995-1-1:2004 [7, 15] accounts for both brittle failure modes and scaling effects from statistics, whereas the regressions in Figure 4 only account for the statistical scaling effects. The proposed linear expressions for self-tapping screws in CLT by Plüss and Brandner et al. [20, 1], and Ringhofer et al. [22] in Table 1 are more in line with the results in Figure 4. From Figure 4, there is no evidence that the effective number of fasteners n_{ef} for the stiffness and ductility should follow a power law if brittle failure modes can be excluded, contrary to what Hossain et al. [11] proposed for self-tapping screws in CLT.

From the regressions in Figure 4, the percentile regressions are fairly similar. Thus, it may not be sensible to distinguish the effective number of fasteners n_{ef} for the different quantities of interest. Because the load-carrying capacity R_{u} holds the highest importance in terms of safety assessments, its effective number of fasteners n_{ef} should act as an upper bound if a single expression should be used to cover all the quantities of interest. By averaging the slopes, neglecting the constants in Figure 4, and using $n_{\mathrm{ef}}(R_{\mathrm{u}})$ as an upper bound, the following expressions are obtained for the effective number of fasteners n_{ef} for the mean and 5$^{\mathrm{th}}$- and 95$^{\mathrm{th}}$-percentiles when brittle failure modes are avoided:

$$\text{for } n > 1,\ n_{\mathrm{ef}} : \begin{cases} n_{\mathrm{ef},0.05} = 0.96n, \\ n_{\mathrm{ef,mean}} = 0.98n, \\ n_{\mathrm{ef},0.95} = 0.99n. \end{cases} \tag{6}$$

4.2.4 Stiffness parameters

In Figure 5, violin and box plots of normalized stiffness parameters $x\frac{\{K_{\mathrm{s,u}}, K_{\mathrm{y}}\}}{K_{\mathrm{y,mean}}}$ are presented. The box plots are organized from left to right with increasing number of fasteners $n \in [1, 3, 5, 10, 15, 30, 60, 90]$. With an increasing number of fasteners n, the relative scatter decreases, which can also be observed from Figure 3. For smaller x in $x\frac{\{K_{\mathrm{s,u}}, K_{\mathrm{y}}\}}{K_{\mathrm{y,mean}}}$, the scatter is generally also smaller as long as the secant does not surpass the maximum load-carrying capacity R_{u}. This indicates that the smallest uncertainty in the stiffness can be obtained for a secant from zero until the maximum load-carrying capacity R_{u}.

Currently, EN 1995-1-1:2004 [7] assumes an ultimate slip modulus $K_{\mathrm{u}} = \frac{2}{3}K_{\mathrm{ser}}$, which corre-

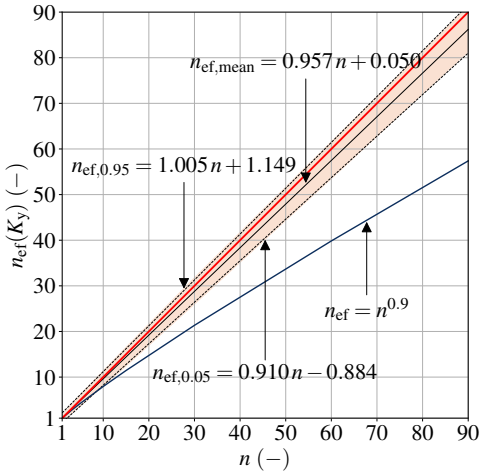

(a) Elastic stiffness K_{y}

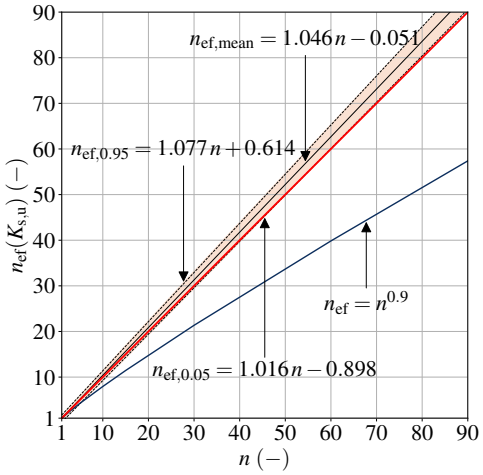

(b) Load-carrying secant stiffness $K_{\text{s,u}}$.

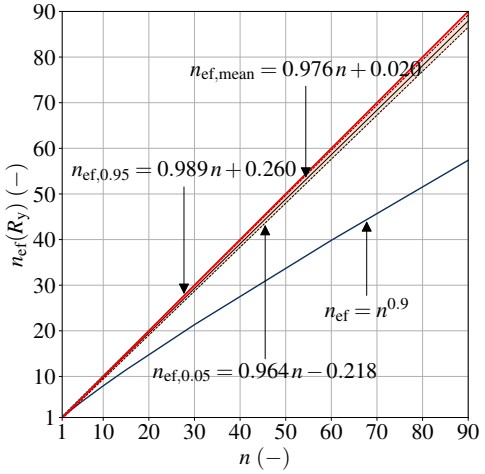

(c) Yield capacity R_{y}.

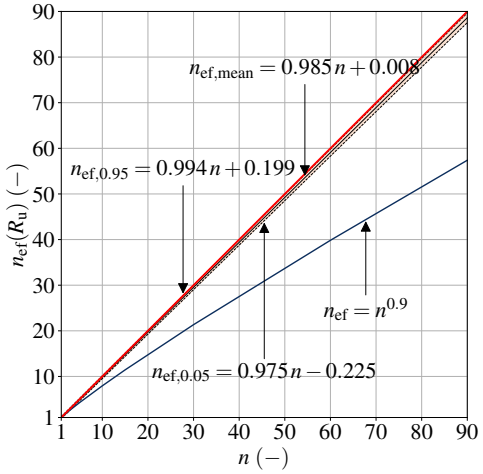

(d) Load-carrying capacity R_{u}.

Figure 4: Parity plots of the effective number of fasteners $n_{\text{ef}}(P)$ and the number of fasteners n for $P \in [K_{\text{y}}, K_{\text{s,u}}, R_{\text{y}}, R_{\text{u}}]$. The red line is the identity line, shaded area the 90 % confidence interval, dashed lines regressions of the 5$^{\text{th}}$- and 95$^{\text{th}}$-percentiles of the effective number of fasteners $n_{\text{ef},\{0.05,0.95\}}$, black solid line regression of the mean effective number of fasteners $n_{\text{ef,mean}}$, and the blue solid line the effective number of fasteners $n_{\text{ef}} = n^{0.9}$ according to EN 1995-1-1:2004 [7].

sponds to $\frac{K_{\text{s,u}}}{K_{\text{y,mean}}} = \frac{4}{6}\frac{K_{\text{y}}}{K_{\text{y,mean}}}$ in Figure 5. When compared with the secant to the maximum load-carrying capacity $\frac{K_{\text{s,u}}}{K_{\text{y,mean}}}$, the simplification in EN 1995-1-1:2004 [7] is too stiff if $K_{\text{s,u}}$ should target the maximum load-carrying capacity R_{u}. If keeping a similar format of $K_{\text{s,u}} = xK_{\text{y}}$ is desirable, then $x \doteq \frac{1}{6}$ is more appropriate. Furthermore, the scatter for $x \doteq \frac{1}{6}$ is much smaller than for $x \doteq \frac{2}{3}$.

The secants xK_{y} are shown with normalized resistance curves $R(\delta)/R_{\text{u}}$ in Figure 3c and Figure 3d. The ultimate secant $K_{\text{u}} = \frac{2}{3}K_{\text{ser}}$ in EN 1995-1-1:2004 [7] was derived by Ehlbeck [4] in relation to a load $R(\delta)$ at $\delta \in [0.5, 1]$ mm such that $K_{1\text{ mm}} = \frac{2}{3}K_{0.5\text{ mm}}$ [12]. However, these displacement limits [4] would still remain in the elastic range in Figure 3c and Figure 3d. Moreover, it is unclear if $x = \frac{2}{3}$ targets the maximum capacity R_{u}, capacity at failure $0.80R_{\text{u}}$, or another point [12]. With the

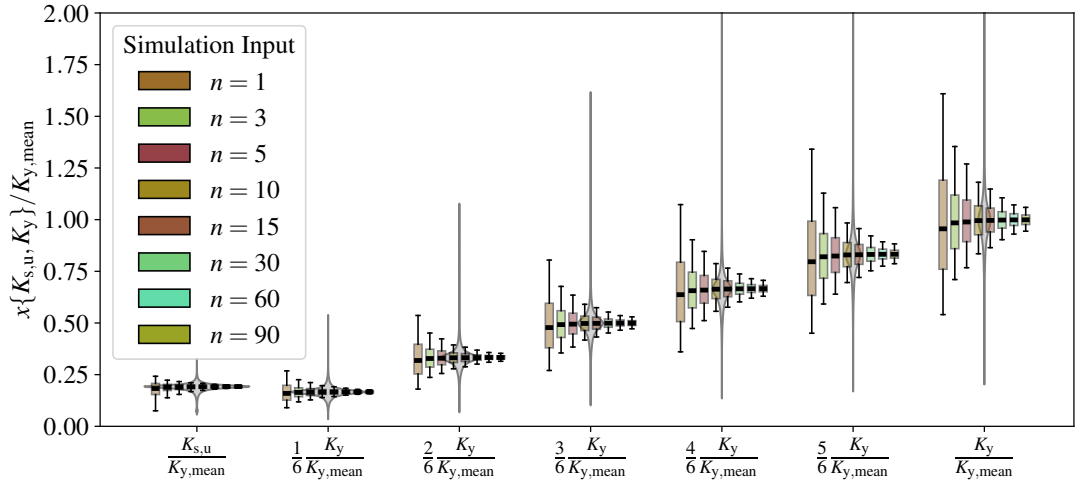

Figure 5: Violin plots and box plots of normalized stiffness ratios $\frac{K_x}{K_{y,mean}}$ for different numbers of fasteners n in the connection. In the box plots, the edges of the box are the 25th and 75th percentile, horizontal line inside the box is the median, and the outer whiskers are the 5th and 95th percentiles.

rigid-plastic assumption in the EYM [14, 18], more mechanically coherent stiffnesses are:

$$K_{s,u} = \frac{1}{6}K_y \quad \vee \quad K_{s,u} = \frac{1}{3}K_y. \tag{7}$$

The consequences of using Equation 7 over $K_u = \frac{2}{3}K_{ser}$ are more compliant connections that attract less loading, but inherits a larger energy-dissipation capacity. For the connections with fastener diameter $d = 10\,\text{mm}$ [19], δ at $x \in [\frac{1}{6}, \frac{1}{3}]$ correspond to $6.1 \leq \delta \leq 12.8\,\text{mm}$, or $0.6 \leq \frac{\delta}{d} \leq 1.3$. This is much greater than the limits of $0.1 \lesssim \frac{\delta}{d} \lesssim 0.2$ by DIN 1052:1988 [12]. Large fastener displacements δ may have a negative influence on neighbouring fasteners, potentially leading to premature brittle failures. As such, $x = \frac{1}{6} \vee x = \frac{1}{3}$ may warrant stricter prescriptive minimum spacing requirements a_1 or explicit checks on brittle failure modes that account for the spacings between the fasteners. Furthermore, $x = \frac{1}{6} \vee \frac{1}{3}$ may lead to such low connection stiffnesses that the ductility may not be mobilized because of second order effects or the mobilization of non-structural components.

4.2.5 Brittle failure modes

In this study, brittle failure modes were not considered. However, a natural extension is to include brittle failure modes and the different failure modes on the fastener level. This can be done by building on the work by Köhler [17]. The group effects that trigger brittle failure modes should be treated separately from the group effects that arise from the statistical effects to ensure mechanical transparency and undesirable non-conservative relations that are present in the current version of EN 1995-1-1:2004 [7]. Such an approach may also result in a more coherent reliability across the relevant failure modes.

5 CONCLUSION

Mechanical and probabilistic modelling were used to assess system effects in laterally-loaded ductile multi-fastener timber connections. System effects result in a characteristic effective number of fasteners $n_{ef,0.05} = 0.96n$ for the stiffnesses and capacities and a reduction in scatter with more fasteners.

Conversely, EN 1995-1-1:2004 follows a power law $n_{\mathrm{ef}} = n^{0.9}$ that includes brittle failure modes.

The secant modulus $K_{\mathrm{s,u}}$ is better represented with $K_{\mathrm{s,u}} = \frac{1}{6}K_{\mathrm{y}}$ than $K_{\mathrm{s,u}} = \frac{2}{3}K_{\mathrm{y}}$ in EN 1995-1-1:2004. $K_{\mathrm{s,u}} = \frac{1}{6}K_{\mathrm{y}}$ causes softer connections that attract less load and enable more energy dissipation, but requires larger deformations that may trigger brittle failure modes. This can be mitigated by stricter spacing requirements and explicit checks on brittle failure modes. Nonetheless, $K_{\mathrm{s,u}} = \frac{1}{6}K_{\mathrm{y}}$ may lead to larger second order effects or the unintended activation of non-structural components.

This study was limited to failure mode III in laterally-loaded dowels, excluding brittle failure modes like splitting, row shear, block shear, or net tension failure. Future work should incorporate these failure modes and distinguish between group effects from statistics and mechanics. This is important for more mechanically transparent design rules and coherent reliability levels.

ACKNOWLEDGEMENTS

The authors gratefully acknowledge the financial support provided by the Swiss National Science Foundation SNSF and Formas - a Swedish Research Council for Sustainable Development in the project *RelyConnect - Reliable and high-performance modern timber structures with modern connections* (SNSF grant no. 220112, Formas grant no. 2023-01603).

REFERENCES

[1] R. Brandner, G. Flatscher, A. Ringhofer, G. Schickhofer, and A. Thiel. Cross laminated timber (CLT): overview and development. *European Journal of Wood and Wood Products*, 74(3):331–351, 5 2016.

[2] A. S. Cao, P. Palma, and A. Frangi. Multi-scale hysteretic model of laterally loaded timber connections with dowel-type fasteners. In J. F. Silva Gomes, editor, *20th International Conference on Experimental Mechanics (ICEM20)*, pages 915–926, Porto, Portugal, 7 2023. INEGI-FEUP.

[3] H. E. Daniels. The statistical theory of the strength of bundles of threads, Part I. *Proceedings of the Royal Society A*, 183(995), 1945.

[4] J. Ehlbeck. Load-carrying capacity and deformation characteristics of nailed joints. In *CIB-W18 Meeting Twelve*, Bordeaux, France, 1979.

[5] J. Ehlbeck and H. Werner. Untersuchungen über die Tragfähigkeit von Stabdübelverbindungen. *Holz als Roh- und Werkstoff*, 45:281–288, 1988.

[6] European Committee for Standardization. EN 26891:1991. Timber structures; joints made with mechanical fasteners; general principles for the determination of strength and deformation characteristics (ISO 6891:1983). Technical report, European Committee for Standardization, Brussels, Belgium, 1991.

[7] European Committee for Standardization. EN 1995-1-1:2004. Eurocode 5: Design of timber structures - Part 1-1: General - Common rules and rules for buildings. Technical report, European Committee for Standardization, Brussels, Belgium, 2004.

[8] European Committee for Standardization. EN 12512:2001 + A1:2005. Timber structures - Test methods - Cyclic testing of joints made with mechanical fasteners. Technical report, European Committee for Standardization, Brussels, 2005.

[9] E. Gehri. Design of joints and frame corners using dowel-type fasteners. In R. Görlacher, editor, *CIB-W18 Meeting Twenty-Nine*, Bordeaux, France, 8 1996. Lehrstuhl fur lngenieurholzbau und Baukonstruktionen, Universitat Karlsruhe.

[10] S. Gollwitzer and R. Rackwitz. On the reliability of Daniels systems. *Structural Safety*, 7(2-4):229–243, 1990.

[11] A. Hossain, M. Popovski, and T. Tannert. Group Effects for Shear Connections with Self-Tapping Screws in CLT. *Journal of Structural Engineering*, 145(8), 8 2019.

[12] R. Jockwer, D. Caprio, and A. Jorissen. Evaluation of parameters influencing the load-deformation behaviour of connections with laterally loaded dowel-type fasteners. *Wood Material Science and Engineering*, 17(1):6–19, 2022.

[13] R. Jockwer, G. Fink, and J. Köhler. Assessment of the failure behaviour and reliability of timber connections with multiple dowel-type fasteners. *Engineering Structures*, 172:76–84, 10 2018.

[14] K. W. Johansen. Theory of timber connections. *IABSE publications*, 9:249–262, 1949.

[15] A. Jorissen. *Double shear timber connections with dowel type fasteners*. PhD thesis, TU Delft, 1998.

[16] A. Jorissen and M. Fragiacomo. General notes on ductility in timber structures. *Engineering Structures*, 33(11):2987–2997, 11 2011.

[17] J. Köhler. A probabilistic framework for the reliability assessment of connections with dowel type fasteners. In R. Görlacher, editor, *CIB - W18, Meeting thirty-eight*, Karlsruhe, Germany, 8 2005. Lehrstuhl fur lngenieurholzbau und Baukonstruktionen, Universitat Karlsruhe.

[18] A. Meyer. Die Tragfähigkeit von Nagelverbindungen bei statischer Belastung. *Holz als Roh- und Werkstoff*, 15(2):96–109, 2 1957.

[19] P. Palma and J. Wydler. Dataset with results of multi-scale experiments on timber connections [Data set], 1 2024.

[20] Y. Plüss and R. Brandner. Untersuchungen zum Tragverhalten von axial beanspruchten Schraubengruppen in der Schmalseite von Brettsperrholz (BSP). In *Internationales Holzbau-Forum IHF 2014*, Garmisch-Partenkirchen, Germany, 2014.

[21] R. M. Richard and B. J. Abbott. Versatile Elastic-Plastic Stress-Strain Formula. *Journal of the Engineering Mechanics Division*, 101(4):511–515, 8 1975.

[22] A. Ringhofer, R. Brandner, and H. J. Blaß. Cross laminated timber (CLT): Design approaches for dowel-type fasteners and connections, 9 2018.

[23] VTT Technical Research Centre of Finland. VTT Certificate no. 184/03. Kerto-S and Kerto-Q Structural laminated veneer lumber. Technical report, VTT Technical Research Centre of Finland, Espoo, Finland, 2009.

[24] M. Yurrita and J. M. Cabrero. On the need of distinguishing ductile and brittle failure modes in timber connections with dowel-type fasteners. *Engineering Structures*, 242, 9 2021.